Available online at www.sciencedirect.com
ScienceDirect
Journal of Sound and Vibration 303 (2007) 575–595
JOURNAL OF SOUND AND VIBRATION
www.elsevier.com/locate/jsvi

# Studies on fluid-filled and submerged cylindrical shells with constrained viscoelastic layer

B. Vamsi Krishna*, N. Ganesan

*Machine Design Section, Department of Mechanical Engineering, Indian Institute of Technology Madras, Chennai 600 036, India*

Received 8 January 2007; accepted 16 January 2007
Available online 27 March 2007

**Abstract**

Conventional cylindrical shells (made of isotropic materials) filled with or submerged in fluid have been analysed historically by using closed-form solutions or by semi-analytical method. However, these shells suffer from a serious disadvantage of not having sufficient damping, which is crucial in controlling the response of the structure during severe vibrations. One practical way of reducing response levels is by using shells with viscoelastic treatment that would result in increased damping. Previous work in this area was mostly limited to study problems whose mathematical formulation was amenable to closed-form solution or semi-analytical method. In some cases researchers resorted to experimental studies. Further, almost all previous studies were limited to lower circumferential modes and to first axial mode only. In the present paper, the method proposed overcomes most of the limitations suffered by adopting the different approaches suggested in literature. The method consists of treating fluid domain with Bessel function approach and shell domain based on first-order shear deformation theory. The present approach obviates the discretisation of liquid domain thus reducing the computation time. A computer program is developed based on the proposed method and results are compared with previous works of various researchers. A good correlation is observed for all the case studies done. Hence, it is claimed that the present approach is more universal for analysing fluid-filled or submerged shells or both. Detailed parametric studies are carried out on both conventional and viscoelastic cylindrical shells.
© 2007 Elsevier Ltd. All rights reserved.

## 1. Introduction

Cylindrical shells, either fluid-filled or submerged in fluid, find wide engineering applications—liquid storage tanks, liquid propellants and submarines, nuclear reactors, are some typical examples. The liquid has a considerable effect on the free vibration behaviour of the structure and hence it is imperative to study the influence of the same on the free vibration behaviour of the structure. Frequency analysis of the above systems has been of a great interest and a challenging task. However, these conventional structures are more vulnerable as they lack sufficient amount of damping in the system. It is felt that an attempt in the direction of increasing damping values with the use of constrained layer damping would be highly beneficial. However,

*Corresponding author.
*E-mail address:* vamsikrishna.balla@gmail.com (B. Vamsi Krishna).

0022-460X/$ - see front matter © 2007 Elsevier Ltd. All rights reserved.
doi:10.1016/j.jsv.2007.01.009

**Nomenclature**

| | |
|---|---|
| [ADM] | added mass matrix |
| **[B]** | strain matrix |
| **[D]** | elasticity matrix |
| $E$ | Young's modulus |
| $G$ | shear modulus |
| $g$ | acceleration due to gravity |
| $H$ | height of liquid |
| $I_n$ | modified Bessel Function |
| $[\mathbf{K}_e]$ | elemental stiffness matrix |
| $m$ | circumferential mode |
| $[\mathbf{m}_e]$ | elemental mass matrix |
| $\hat{N}$ | trial functions |
| $N_i$ | shape functions |
| $n$ | axial mode |
| $R_\theta$ | radius of curvature in the $\theta$ direction |
| $s, \theta, z$ | coordinate directions |
| $t_c$ | thickness of core |
| $t_f$ | individual thickness of facing |
| $u, v, w$ | displacement in the $s$, $\theta$, $z$ directions, respectively |
| $v$ | Poisson's ratio |
| $\rho_s$ | mass density of structure |
| $\rho_l$ | mass density of liquid |

very little literature is available that treat viscoelastic shell structure interacting with fluid. Hence, in the present paper, studies are done on viscoelastic cylindrical shells to learn the improvement in damping values.

The analysis of vertical fluid-filled cylindrical shells was done by Haroun [1] using finite element for shell structure and boundary solution technique for fluid continuum. He had studied the seismic response of the above structure by considering zeroth and first circumferential mode. Gupta and Hutchnison [2] studied the problem by using semi-analytical finite-element approach for both fluid and shell domain. However, there is not much literature available on viscoelastic fluid-filled shells except the one carried out by Ramasamy and Ganesan [3]. They had analysed the system by using semi-analytical finite element for both structure and liquid domain. In the present paper, liquid storage tank systems are modelled by using viscoelastic material. This enabled to incorporate passive damping thus improving the dynamic characteristics of the structure. The present paper deals with viscoelastic fluid-filled shells using the Bessel function approach suggested by Haroun [1]. This approach consists of treating the shell with finite elements and liquid domain as a continuum thus in turn resulting in the reduction of computational time. It is found that no researchers have used the Bessel function approach to evaluate the natural frequencies of fluid-filled cylindrical shells for higher circumferential modes. The present paper discusses the results on two oil containers that are dealt in the literature namely short shell and long shell. The rationale behind the selection of above structures for the present study is to enable the comparison of improvement in the damping values with respect to those published earlier in the literature. However, the frequency can be normalised and compared to any other shell with different dimensions by using the formula $\mathbf{\Omega} = \rho t R\omega^2/E$. According to best of the authors' knowledge, there are no studies on higher axial modes for these systems. The present method can be easily extended to analyse the submerged cylindrical shells by changing the fluid potential. The results are found to correlate very well with those published by Chiba [4]. According to the best of the authors' knowledge literature on submerged vertical viscoelastic shells is very limited. The present paper discusses the results for vertical viscoelastic submerged cylindrical shells. Numerical results and detailed discussions are produced on the free vibration frequencies and the loss factors of the constrained viscoelastic shell with isotropic and orthotropic facings.

## 2. Structural finite element

Ramasamy and Ganesan [3] have developed a general shell finite element for viscoelastic shells based on the displacement field proposed by Wilkins et al. [5]. Fig. 1 shows the schematic of the viscoelastic shell structure, consisting of a core viscoelastic layer sandwiched between two facing layers. The extreme layers of the shell are called facings, and their individual thickness is denoted by $t_f$. The central portion of the shell is a constrained viscoelastic layer, which is called core, and the thickness of the same is denoted by $t_c$.

For the core layer the displacement relations are assumed to be

$$u^c = u_o + z\psi_s, \quad v^c = v_o + z\psi_\theta, \quad w^c = w_o, \tag{1}$$

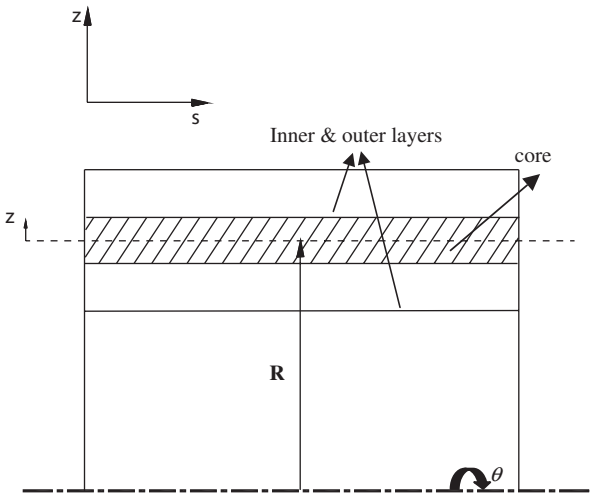


Fig. 1. Schematics of a constrained viscoelastic layer.

where $u^c$, $v^c$, and $w^c$ are the total displacements in the $s$, $\theta$, and $z$ directions and are defined in terms of the middle surface displacements $u_o$, $v_o$, and $w_o$ and the angles, $\psi_s$ and $\psi_\theta$, are rotations of normal to the middle surface in the meridional and circumferential directions. For the core these angles are denoted by $\psi_s$, $\psi_\theta$ and for the facings the angles are denoted as $\phi_s$ and $\phi_\theta$. The displacement relations for outer and inner facing are, respectively

$$u^{\mathrm{fo}}, u^{\mathrm{fi}} = u_o \pm h\psi_s + (z \pm h)\phi_s, \quad v^{\mathrm{fo}}, v^{\mathrm{fi}} = v_o \pm h\psi_\theta + (z \pm h)\phi_\theta, \quad w^{\mathrm{fo}}, w^{\mathrm{fi}} = w_{\mathrm{o}}. \tag{2}$$

Here '$z$' denotes the distance from the middle surface of the shell, '$h$' is half the core thickness and $R$ is the radius of the shell with respect to the axis. The strain–displacement relations for the core then become

$$k = 1 \Big/ \left(1 + \frac{z}{R_\theta}\right), \tag{3}$$

$$\varepsilon^c_{ss} = \left(\frac{\partial u_0}{\partial s} + z\frac{\partial \psi_s}{\partial s}\right), \quad \varepsilon^c_{zz} = 0, \tag{4}$$

$$\varepsilon^c_{\theta\theta} = k\left[\frac{1}{r}\frac{\partial v_0}{\partial \theta} + \frac{w_0}{r} + z\left(\frac{1}{r}\frac{\partial \psi_\theta}{\partial \theta}\right)\right], \tag{5}$$

$$\gamma^c_{s\theta} = k\left[\frac{1}{r}\frac{\partial u_0}{\partial \theta} + \frac{\partial v_0}{\partial s} + z\left(\frac{1}{r}\frac{\partial \psi_s}{\partial \theta} + \frac{\partial \psi_\theta}{\partial s}\right)\right], \tag{6}$$

$$\gamma^c_{sz} = k\left[\psi_s + \frac{\partial w_0}{\partial s}\right], \tag{7}$$

$$\gamma^c_{\theta z} = k\left[\psi_\theta - \frac{v_0}{r} + \frac{1}{r}\frac{\partial w_0}{\partial \theta} + z\left(-\frac{\psi_\theta}{r}\right)\right]. \tag{8}$$

For the inner and outer facings these relations are

$$\varepsilon^o_{ss}, \varepsilon^i_{ss} = k\left[\frac{\partial u_0}{\partial s} \pm h\frac{\partial \psi_s}{\partial s} + (z \mp h)\frac{\partial \phi_s}{\partial s}\right], \quad \varepsilon^o_{zz}, \varepsilon^i_{zz} = 0, \tag{9}$$

$$\varepsilon^o_{\theta\theta}, \varepsilon^i_{\theta\theta} = k\left[\frac{1}{r}\frac{\partial v_0}{\partial \theta} + \frac{w_0}{r} \pm h\left(\frac{1}{r}\frac{\partial \psi_\theta}{\partial \theta}\right) + (z \mp h)\left(\frac{1}{r}\frac{\partial \phi_\theta}{\partial \theta}\right)\right], \tag{10}$$

$$\gamma_{s\theta}^{o},\gamma_{s\theta}^{i}=k\left[\frac{1}{r}\frac{\partial u_0}{\partial\theta}+\frac{\partial v_0}{\partial s}\pm h\left(\frac{1}{r}\frac{\partial\psi_s}{\partial\theta}+\frac{\partial\psi_\theta}{\partial s}\right)+(z\mp h)\left(\frac{1}{r}\frac{\partial\phi_s}{\partial\theta}+\frac{\partial\phi_\theta}{\partial s}\right)\right], \tag{11}$$

$$\gamma_{sz}^{o}\gamma_{sz}^{i}=k\left[\phi_s+\frac{\partial w_0}{\partial s}\right], \tag{12}$$

$$\gamma_{\theta z}^{o},\gamma_{\theta z}^{i}=k\left[\phi_\theta-\frac{v_0}{r}+\frac{1}{r}\frac{\partial w_0}{\partial\theta}\pm h\left(-\frac{\psi_\theta}{r}\right)+(z\mp h)\left(-\frac{\phi_\theta}{r}\right)\right]. \tag{13}$$

It is clear from Eqs. (3)–(13) that the degrees of freedom are $u_0$, $v_0$, $w_0$, $\psi_s$, $\psi_\theta$, $\phi_s$, and $\phi_\theta$. In semi-analytical formulation the circumferential variation of the seven variables (along $\theta$) are expressed as a Fourier series as shown below:

$$\begin{Bmatrix} u_0\\ v_0\\ w_0\\ \psi_s\\ \psi_\theta\\ \phi_s\\ \phi_\theta \end{Bmatrix}=\sum_{i=1}^{3}\sum_{m=0}^{\infty}[\bar{\theta}]\begin{Bmatrix} N_i\ u_{0m,i}\\ N_i\ v_{0m,i}\\ N_i\ w_{0m,i}\\ N_i\ \psi_{sm,i}\\ N_i\ \psi_{\theta m,i}\\ N_i\ \phi_{sm,i}\\ N_i\ \phi_{\theta m,i} \end{Bmatrix}, \tag{14}$$

where $[\bar{\theta}]$ is defined as follows:

$$[\bar{\theta}]=\begin{bmatrix} c & & & & & & \\ & s & & & & & \\ & & c & & & & \\ & & & c & & & \\ & & & & s & & \\ & & & & & s & \\ & & & & & & c \end{bmatrix}, \tag{15}$$

where $c=\cos m\theta$, $s=\sin m\theta$, where '$m$' is circumferential mode number, $N_i$ are the shape functions used in finite-element formulation given by $N_1=(\xi^2-\xi)/2$, $N_2=1-\xi^2$, $N_3=(\xi^2-\xi)/2$ where $\xi=s/l$, is the isoparametric axial coordinate and $l$ is the length of the element. The elemental displacement vector with three nodes and seven degree of freedom per node is then:

$$\{\mathbf{u}_e\}^{\mathrm{T}}=\{u_{o1},v_{o1},w_{o1},\psi_{s1},\psi_{\theta1},\phi_{s1},\phi_{\theta1},u_{o2},v_{o2},w_{o2},\psi_{s2},\ldots,w_{o3},\psi_{s3},\psi_{\theta3},\phi_{s3},\phi_{\theta3}\}. \tag{16}$$

The subscripts 1, 2 and 3 denote the three nodes. Now we can write the displacement vector as $\{\mathbf{u}\}=[\mathbf{N}]\{\mathbf{u}_e\}$ where $\{\mathbf{u}\}^{\mathrm{T}}=\begin{Bmatrix} u^c & v^c & w^c \end{Bmatrix}$ for the core and $\{\mathbf{u}\}^{\mathrm{T}}=\begin{Bmatrix} u^{\mathrm{fo/fi}} & v^{\mathrm{fo/fi}} & w^{\mathrm{fo/fi}} \end{Bmatrix}$ for the facings. The strain vectors can be represented as $\{\varepsilon\}=\begin{Bmatrix} \varepsilon_{ss} & \varepsilon_{\theta\theta} & \gamma_{s\theta} & \gamma_{\theta z} & \gamma_{sz} \end{Bmatrix}=[\mathbf{B}]\{\mathbf{u}_e\}$ where $[\mathbf{B}]$ is the strain–displacement matrix. The elemental stiffness $[\mathbf{K}_e]$ and mass $[\mathbf{m}_e]$ matrices are then obtained from the following:

$$[\mathbf{K}_e]=\int_v[\mathbf{B}]^{\mathrm{T}}[\mathbf{D}][\mathbf{B}]\,\mathrm{d}v\quad[\mathbf{m_e}]=\rho_s\int_v[\mathbf{N}]^{\mathrm{T}}[\mathbf{N}]\,\mathrm{d}v, \tag{17}$$

where

$$[\mathbf{D}]=\begin{bmatrix} \bar{\mathbf{Q}}_{11} & \bar{\mathbf{Q}}_{12} & \bar{\mathbf{Q}}_{13} & 0 & 0\\ & \bar{\mathbf{Q}}_{22} & \bar{\mathbf{Q}}_{23} & 0 & 0\\ & & \bar{\mathbf{Q}}_{33} & 0 & 0\\ \text{Sym.} & & & \bar{\mathbf{Q}}_{44} & 0\\ & & & & \bar{\mathbf{Q}}_{55} \end{bmatrix},$$

$\bar{\mathbf{Q}} = [\mathbf{T}]^{\mathrm{T}}[\mathbf{Q}][\mathbf{T}]$ is the transformed elasticity matrix in global coordinates, [**Q**] is the elasticity matrix in the material coordinates and [**T**] is the standard transformation matrix to convert to the global coordinates. Numerical integration using Gauss quadrature scheme is carried out for Eq. (17). If the same material is used for all the three layers, the above formulation will reduce to first-order shear deformation theory.

## 3. Fluid formulation

The finite-element method is very useful for analysing fluid domain with a great convenience in dealing with fluid–structure interaction problems. However, for analysing the present problem, it is advantageous to treat the liquid region as a continuum by the boundary solution technique and to model the elastic shell by finite elements. In essence, the boundary solution technique consists of choosing a set of trial functions that satisfies, the differential equation throughout the domain; and consequently, only the boundary conditions have to be satisfied in an average integral sense. As the boundary solution technique involves only the boundary, the number of unknowns can be much less than those of a standard finite-element analysis. However, the boundary solution technique is limited to simple, homogeneous and linear problems for which suitable trial functions can be identified.

### 3.1. Equations governing liquid motion

A typical geometry representation of the cylindrical shell filled with fluid is shown in Fig. 2. For irrotational flow of an incompressible inviscid liquid, the velocity potential, $\phi(r, \theta, z)$ satisfies the Laplace equation

$$\nabla^2\phi = 0 \tag{18}$$

in the region occupied by the liquid ($0 \leqslant r \leqslant R$, $0 \leqslant \theta \leqslant 2\pi$, $0 \leqslant z \leqslant H$). Since, the velocity vector of the liquid is the gradient of the velocity potential, the liquid-container boundary conditions can be expressed as follows.

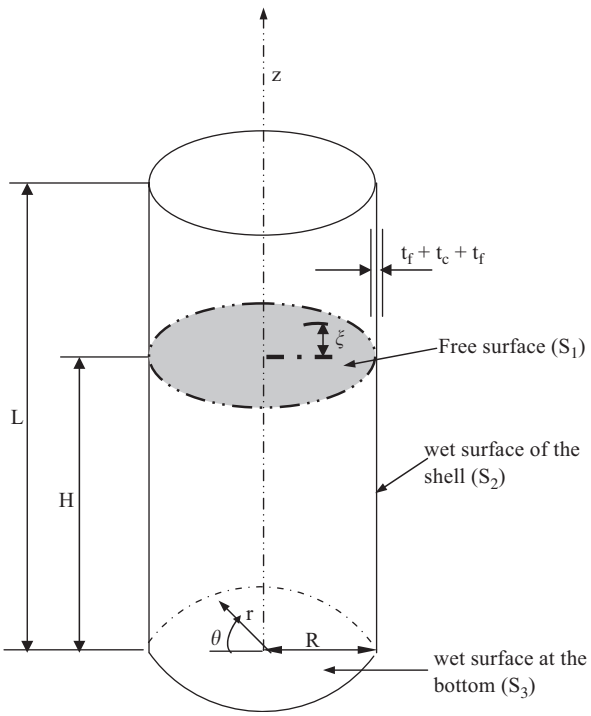


Fig. 2. Schematics of a cylindrical fluid-filled shell.

At the rigid tank bottom, $z = 0$, the liquid velocity in the vertical direction is zero

$$\frac{\partial \phi}{\partial z}(r, \theta, 0, t) = 0. \tag{19}$$

For the liquid adjacent to the wall of the elastic shell, $r = R$, fluid must move radially with the same velocity as the shell, hence

$$\frac{\partial \phi}{\partial r}(R, \theta, z, t) = \frac{\partial w}{\partial t}(\theta, z, t), \tag{20}$$

where $w(\theta, z, t)$ is the shell radial displacement.

At the liquid free surface $z = H + \zeta(r, \theta, t)$, two boundary conditions must be imposed. The kinematic condition states the fluid particle on the free surface will always remain on the free surface. The other boundary condition specifies that the pressure on the free surface is zero. By considering only small-amplitude waves, the free surface boundary conditions become

$$\begin{aligned} &\frac{\partial \phi}{\partial z}(R, \theta, z, t) = \frac{\partial \xi}{\partial t}(r, \theta, t), \\ &\rho_l \frac{\partial \phi}{\partial t}(R, \theta, H, t) + \rho_l g \xi(r, \theta, t) = 0, \end{aligned} \tag{21}$$

where $\rho_l$ is mass density of liquid and '$g$' is the acceleration due to gravity.

Following the variational formulation presented by Luke [6], the appropriate functional for a liquid having a free surface is given by

$$J_c(\phi, \xi) = \int_{t_1}^{t_2} L_c(\phi, \xi)\, \mathrm{d}t, \tag{22}$$

where $L_c$ is the complementary Lagrangian functional given by

$$L_c(\phi, \xi) = -\frac{\rho_l}{2} \int_V (\nabla \phi \nabla \phi)\, \mathrm{d}v + \rho_l \int_{S_1} \left( \phi \xi - \frac{g \xi^2}{2} \right) \mathrm{d}s + \int_{S_2} \phi \dot{w}\, \mathrm{d}s \tag{23}$$

in which $V$ indicates the volume occupied by the liquid. By requiring that the first variation of $J_c$ be identically zero, the Laplace equation and the linear boundary conditions can be obtained.

### 3.2. Variational formulation

On combining the above equations the variational functional for the free lateral vibration of the liquid-shell system can be expressed as

$$J(u, v, w, \phi, \xi) = \int_{t_1}^{t_2} \left\{ \begin{array}{c} T(\dot{u}, \dot{v}, \dot{w}) - U(u, v, w) - \frac{\rho_l}{2} \int_V (\nabla \phi \nabla \phi) \\ + \rho_l \int_{S_1} \left( \xi \phi - \frac{g \xi^2}{2} \right) + \rho_l \int_{S_2} w \dot{\phi}\, \mathrm{d}s \end{array} \right\} \mathrm{d}t. \tag{24}$$

In the basic analysis, only impulsive pressure of the liquid is considered; and therefore, the shell vibrational motion becomes independent of the free surface motion. Given this assumption, the functional $J$ takes the form

$$J(u, v, w, \phi, \xi) = \int_{t_1}^{t_2} \left\{ T(\dot{u}, \dot{v}, \dot{w}) - U(u, v, w) - \frac{\rho_l}{2} \int_V (\nabla \phi \nabla \phi) + \rho_l \int_{S_2} w \dot{\phi}\, \mathrm{d}s \right\} \mathrm{d}t. \tag{25}$$

Once a set of trial functions $\hat{N}_i(r, \theta, z)$, which are solutions of the Laplace equation, are identified, then one can assume that

$$\phi(r, \theta, z, t) = \sum_{i=1}^{I} A_i(t) \hat{N}_i(r, \theta, z), \tag{26}$$

where $I$ is the number of trial functions, and $\hat{N}_i(r,\theta,z)$ could be written as

$$\hat{N}_i(r,\theta,z) = \sum_{n=1}^{\infty} I_n(\alpha_i r)\cos(\alpha_i z)\cos(n\theta), \tag{27}$$

where $I_n$ is modified Bessel Function

$$\alpha_i = \frac{(2i-1)\pi}{2H} \quad \text{and} \quad i = 1,2\ldots I. \tag{28}$$

Chosen trial function satisfy the boundary conditions along $S_1$ and along $S_3$, then

$$\frac{\rho_l}{2}\int_S \phi\frac{\partial\phi}{\partial v}\,\mathrm{d}s = \frac{\rho_l}{2}\int_{S_2}\phi\frac{\partial\phi}{\partial v}\,\mathrm{d}s = \frac{1}{2}\{A\}^{\mathrm{T}}[C]\{A\}, \tag{29}$$

where $[C]$ is a diagonal matrix whose elements are given by

$$C_{ii} = \frac{\pi R\rho_l\alpha_i H}{2} I_n(\alpha_i R)I_n'(\alpha_i R). \tag{30}$$

With the aid of the finite-element model of the shell and the expression of the velocity potential function, the last term of $J$ becomes

$$\rho_l\int_{S_2}\dot{w}\phi\,\mathrm{d}s = \{\dot{q}\}^{\mathrm{T}}[\hat{C}]\{A\}. \tag{31}$$

Inserting these equations into the variational functional, and applying the variational operator yields

$$\begin{aligned}&[M_s]\{\ddot{q}\} + [K_s]\{q\} + [\hat{C}]\{\dot{A}\} = \{0\},\\ &[C]\{A\} - [\hat{C}]^{\mathrm{T}}\{\dot{q}\} = \{0\}.\end{aligned} \tag{32}$$

Since the matrix $[C]$ is non-singular

$$\{A\} = [C]^{-1}[\hat{C}]^{\mathrm{T}}\{\dot{q}\} \tag{33}$$

substituting Eq. (33) into Eq. (32) yields

$$\begin{aligned}&[M_s]\{\ddot{q}\} + [K_s]\{q\} + [\hat{C}][C]^{-1}[\hat{C}]^{\mathrm{T}}\{\ddot{q}\} = \{0\},\\ &([M_s] + [\mathrm{ADM}])\{\ddot{q}\} + [K_s]\{q\} = \{0\},\end{aligned} \tag{34}$$

where [ADM] is added mass matrix due to the effect of the liquid. The matrix [ADM] is symmetric and partially complete. Eq. (34) is solved by using simultaneous iteration to extract complex eigenvalues. These eigenvalues are complex in nature as viscoelastic material properties are taken into account. The square root of real part of the complex eigenvalue gives natural frequency and the ratio of the imaginary to real part of the eigenvalue gives the corresponding loss factor.

The present methodology is extended to submerged shells where subsequent change in spatial velocity potential is made by discarding the modified first kind of Bessel function $I_n$ and by including $K_n$ in Eq. (27) as it must be regular at extreme radius. It should also be noted that both kinds of Bessel functions should be considered for submerged fluid-filled shells.

## 4. Results and discussions

### 4.1. Fluid-filled viscoelastic shells

#### 4.1.1. Validation

The frequency analysis of cylindrical shells filled with fluid can be carried out by using semi-analytical finite element for structure and Bessel function approach for fluid domain. This kind of approach is more efficient compared to the usage of semi-analytical finite-element approach for both structure and fluid. Hence in the present paper, a study is done on viscoelastic fluid-filled shells using this approach and results obtained are compared with those of Ramasamy and Ganesan [3]. The analysis is carried out for a fully filled short

Glass/Epoxy shell with water and whose dimensions are $R = 18.29$, $L = 12.2$, $t = 0.0254$ m. The core is assumed to be made of PVC and its properties are given in the Appendix A. It is assumed that these properties are independent of frequency and temperature. The shell structure is discretised by using 10 finite elements in the axial direction. Ten number of trial functions ($\hat{N}$) were used for analysing liquid domain. The structure is clamped at one end while the other end is free. Table 1 shows the results of a Glass/Epoxy shell with fibre orientation in the axial direction. As can be seen from Table 1, the correlation between the results is good. Viscoelastic shells with circumferential fibre orientation were also analysed and the results are compared with those of Ramasamy et al. in Table 2 and the correlation observed is very good.

#### 4.1.2. Studies on isotropic short and tall shell

The variation of frequency (Hz) and loss factor of a mild steel tank along the circumferential modes for different $t_c/t_f$ (core to facing thickness ratios) ratios is discussed. Fig. 3 shows the variation of frequency versus circumferential mode number of short half-filled and fully filled shells. It is observed from the graph that at lower circumferential modes, for a given mode number, the frequency decreases as the $t_c/t_f$ ratio increases. In general for the shell vibration at lower modes, the membrane effect will be predominant. In contrast, at higher

Table 1
Comparison of the natural frequencies (Hz) of a fully filled short Glass/Epoxy shell with fibre angle 0°

| $m$ | Present approach | | Ramasamy and Ganesan [3] | |
|---|---|---|---|---|
| | Frequency (Hz) | Loss factor | Frequency (Hz) | Loss factor |
| | $t_c/t_f = 1$ | $t_c/t_f = 1$ | $t_c/t_f = 1$ | $t_c/t_f = 1$ |
| 1 | 1.34 | 0.0034 | 1.34 | 0.0031 |
| 2 | 1.20 | 0.0021 | 1.21 | 0.0020 |
| 3 | 1.02 | 0.0016 | 1.01 | 0.0015 |
| 4 | 0.86 | 0.0015 | 0.86 | 0.0014 |
| 5 | 0.75 | 0.0016 | 0.75 | 0.0015 |
| 6 | 0.65 | 0.0017 | 0.65 | 0.0016 |
| 7 | 0.58 | 0.0019 | 0.58 | 0.0018 |
| 8 | 0.53 | 0.0024 | 0.53 | 0.0022 |
| 9 | 0.49 | 0.0031 | 0.49 | 0.0029 |
| 10 | 0.48 | 0.0045 | 0.48 | 0.0041 |

Table 2
Comparison of the natural frequencies (Hz) of fully filled a short Glass/Epoxy shell with fibre angle 90°

| $m$ | Present approach | | Ramasamy and Ganesan [3] | |
|---|---|---|---|---|
| | Frequency (Hz) | Loss factor | Frequency (Hz) | Loss factor |
| | $t_c/t_f = 1$ | $t_c/t_f = 1$ | $t_c/t_f = 1$ | $t_c/t_f = 1$ |
| 1 | 2.17 | 0.0004 | 2.17 | 0.0004 |
| 2 | 1.45 | 0.0005 | 1.45 | 0.0004 |
| 3 | 1.04 | 0.0005 | 1.04 | 0.0005 |
| 4 | 0.79 | 0.0006 | 0.79 | 0.0006 |
| 5 | 0.63 | 0.0009 | 0.63 | 0.0008 |
| 6 | 0.52 | 0.0019 | 0.52 | 0.0017 |
| 7 | 0.47 | 0.0051 | 0.47 | 0.0046 |
| 8 | 0.46 | 0.0114 | 0.46 | 0.0103 |
| 9 | 0.49 | 0.0200 | 0.50 | 0.0181 |
| 10 | 0.56 | 0.0290 | 0.57 | 0.0263 |

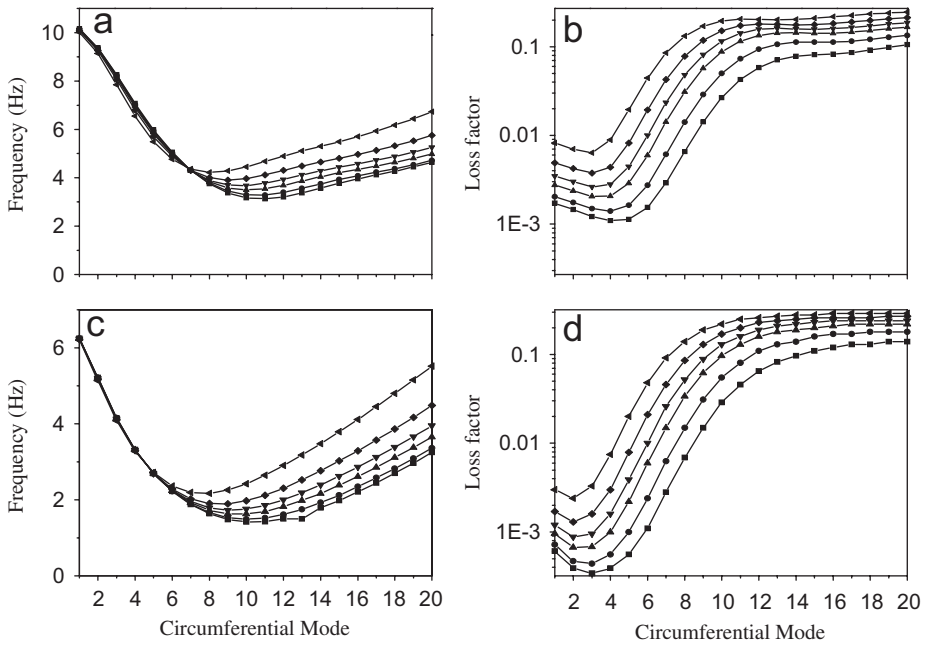


Fig. 3. Plot of frequency (Hz) and loss factor of a short mild steel tank: (a) frequencies of half-filled; (b) loss factors of half-filled; (c) frequencies of fully filled; (d) loss factors of fully filled: —■— $t_c/t_f = 0.5$; —●— $t_c/t_f = 1.0$; —▲— $t_c/t_f = 2.0$; —▼— $t_c/t_f = 3.0$; —◆— $t_c/t_f = 5.0$; —◀— $t_c/t_f = 10.0$.

modes the bending effect will be more predominant. Hence as the $t_c/t_f$ ratio increases, apparently the bending rigidity also increases considerably and such an effect is seen at higher modes. Consequently, the frequencies of the higher modes increase when the $t_c/t_f$ ratio increases. At lower modes mass effects are more predominant when compared to stiffness effects, hence the frequencies decrease at lower modes. The circumferential mode at which the lowest frequency occurs shifts toward lower mode numbers as the $t_c/t_f$ ratio increases.

This is conceived as the increase of $t_c/t_f$ ratio gives more bending rigidity. In case of half-filled and fully filled shells, the same trend is observed. However, the frequencies of half-filled and fully filled shells are considerably different as the added mass effect of the fluid is distinct in both the cases. The frequencies of fully filled and half-filled shells are almost constant for all $t_c/t_f$ ratios at lower circumferential modes. However, the effect of $t_c/t_f$ ratio on the frequency is more pronounced at higher modes.

Fig. 3 also shows that the variation of loss factor versus circumferential mode number of a short half-filled and fully filled shells. The loss factor increases for half-filled and fully filled shells as the $t_c/t_f$ ratio increases. The loss factor increases rapidly up to certain mode number and it becomes almost constant at higher modes. This phenomenon substantiates the fact that passive control is more effective at lower circumferential modes.

Fig. 4 shows the plot of the frequency and loss factor versus circumferential mode number of tall half-filled and fully filled shells. The trend observed is same as in the case of short mild steel tank.

### *4.1.3. Studies on orthotropic short and tall shell*

This section presents the frequencies and loss factors of a tall shell with facings made of Kevlar/Epoxy material. Fig. 5 shows the variation of natural frequency and loss factor of a tall shell made of Kevlar/Epoxy material with axial fibre orientation (fibre angle 0°). The figure shows the results of half-filled and fully filled shells for various values of $t_c/t_f$ ratios. It is observed that there is a little change in frequency of half-filled and fully filled shell at lower circumferential modes as the core to facing thickness ratio increases. Frequency of fluid-filled shells increases at higher modes thus indicating that increase of $t_c/t_f$ ratio has highly appreciable influence on the stiffness of the shell. The damping behaviour of tall shell, as is seen from the figures is that in

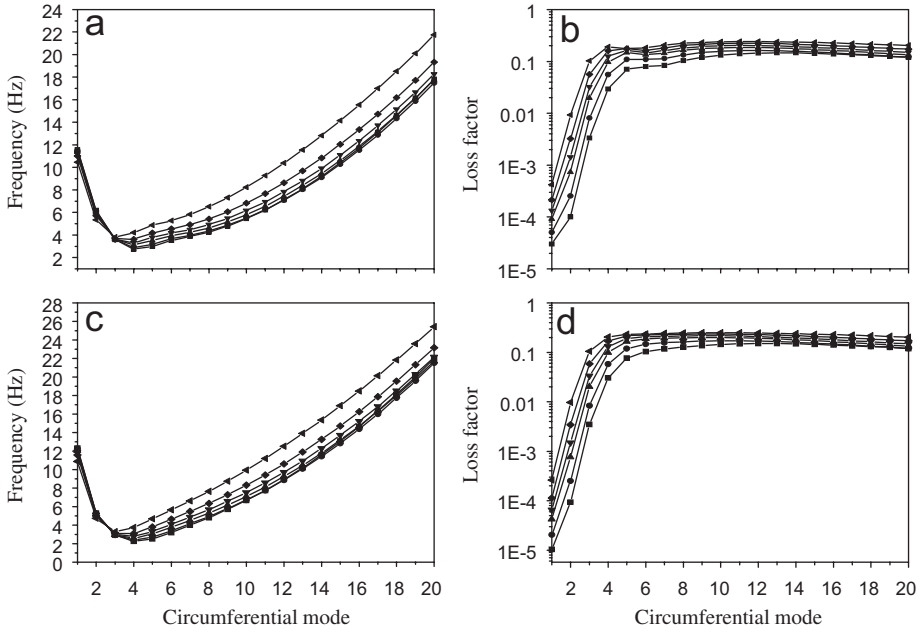


Fig. 4. Plot of frequency (Hz) and loss factor of a long mild steel tank: (a) frequencies of half-filled; (b) loss factors of half-filled; (c) frequencies of fully filled; (d) loss factors of fully filled: —■— $t_c/t_f = 0.5$; —●— $t_c/t_f = 1.0$; —▲— $t_c/t_f = 2.0$; —▼— $t_c/t_f = 3.0$; —♦— $t_c/t_f = 5.0$; —◀— $t_c/t_f = 10.0$.

general at lower circumferential mode number there is no significant change in damping values. This is because of the fact that the membrane effect is more predominant at lower modes and does not appreciably increase the damping of the system.

Fig. 6 shows the plot of frequency and loss factor of a tall Kevlar/Epoxy shell with circumferential fibre orientation (fibre angle 90°). The frequency behaviour of 90° fibre-oriented shell is similar to that of 0° fibre-oriented shells. However, the damping of lower circumferential modes of circumferentially fibre-oriented shell is higher compared to axial fibre-oriented shell. A similar trend in the variation of natural frequency and loss factor of a short shell made of Kevlar/Epoxy material with axial fibre orientation (fibre angle 0°) was observed. The damping values of both half-filled and fully filled shell decreases for fist few circumferential modes and then increases.

The frequency behaviour of short Kevlar/Epoxy shell with 90° fibre orientation shell is similar to that of 0° fibre-oriented shell. However, there is a steep rise in the loss factor with increase in circumferential mode number. However, results of short Kevlar/Epoxy are not presented because of space limitations.

#### *4.1.4. Comparison of frequencies and loss factors for different composite materials with axial fibre orientation*

Tables 3 and 4 give the variation of frequency and loss factor of a short shell with fibre orientation in axial direction under fluid-filled condition for various composite materials. Damping of fluid-filled shells is higher at first bending mode especially when core to facing thickness ratio is five. Hence, the addition of viscoelastic damping may have better effect in fluid-filled shells. In addition, Graphite/Epoxy shells in general seem to have higher damping. Tables 5 and 6 give the variation of frequency and loss factor for different materials under fluid-filled condition for tall tank with axial fibre direction. It is seen that damping at higher modes are quite considerable in case of tall shells.

#### *4.1.5. Frequencies and loss factors of the cylindrical shells for higher axial modes*

In the previous sections, frequencies and loss factors of cylindrical shell are presented for various circumferential modes corresponding to first axial mode only. This section deals with some typical results for higher axial modes of the cylindrical shell with $t_c/t_f = 1$. Fig. 7 shows the variation of frequency and loss

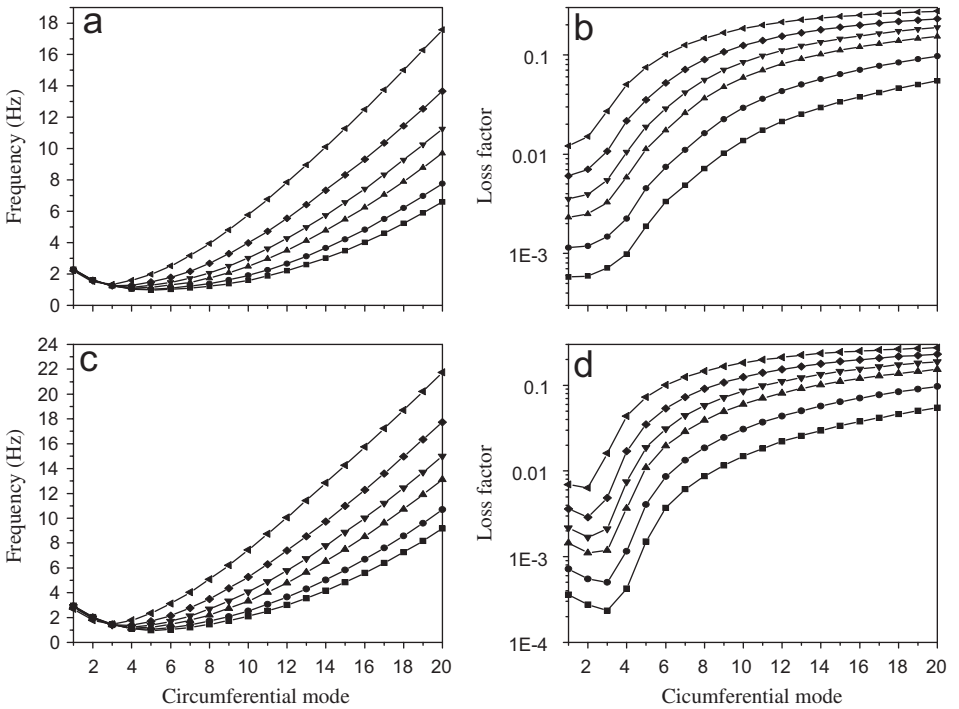


Fig. 5. Plot of frequency (Hz) and loss factor of a long Kevlar/Epoxy tank with fibre angle 0°: (a) frequencies of half-filled; (b) loss factors of half-filled; (c) frequencies of fully filled; (d) loss factors of fully filled: —■— $t_c/t_f = 0.5$; —●— $t_c/t_f = 1.0$; —▲— $t_c/t_f = 2.0$; —▼— $t_c/t_f = 3.0$; —◆— $t_c/t_f = 5.0$; —◀— $t_c/t_f = 10.0$.

factor of a short mild steel cylindrical shell in both half-filled and fully filled conditions with $t_c/t_f = 1$ for higher axial modes. For the first axial mode decreasing–increasing trend of frequency versus circumferential mode number is observed. It can be seen from the figure that the variation of frequency along circumferential mode number reduces as the axial mode number increases. The frequency decreases continuously up to $m = 20$ for the axial modes $n = 3$ and 5. Loss factor of cylindrical shell increases with increase in axial mode number at lower circumferential modes. But at higher circumferential modes, loss factor decreases with increase in axial mode number. Loss factor of the shell does not vary with circumferential mode number for higher axial modes. For axial mode $n = 1$, loss factor of the shell decreases at mode $m = 1$ and then increases. But for other axial modes, loss factor increases continuously with increase in circumferential mode number.

Variation of frequency and loss factor of a tall mild steel cylindrical shell for higher axial modes with $t_c/t_f = 1$ is shown in Fig. 8. The fall in frequency with the increase in circumferential mode number reduces in case of tall shell also, as the axial mode number increases. Loss factors of shell increase with increase in axial mode number for lower circumferential modes and it is vice-versa at higher circumferential modes.

### *4.1.6. Influence of different boundary conditions*

In order to ascertain the validity of the proposed method for other classical boundary conditions like clamped–clamped (CC), clamped–free (CF) and simply supported (SS), a limited study is done. This study gives the influence of boundary conditions for fluid-filled structures. Tables 7 and 8 show the comparison of frequencies and loss factors of short fluid-filled mild steel cylindrical shell with CC, SS and CF boundary conditions for the first axial mode. Comparison of frequencies and loss factors of a tall fully filled mild steel cylindrical shell with CC, SS and CF boundary conditions for the first axial mode is listed in Tables 9 and 10.

The difference in the values of both frequencies and loss factors obtained for shells with different boundary conditions is reckoned. However in the case of short fluid-filled shells, even though there is a considerable difference in frequencies and loss factors at lower circumferential modes between different boundary conditions, the difference becomes less at higher circumferential modes. In the case

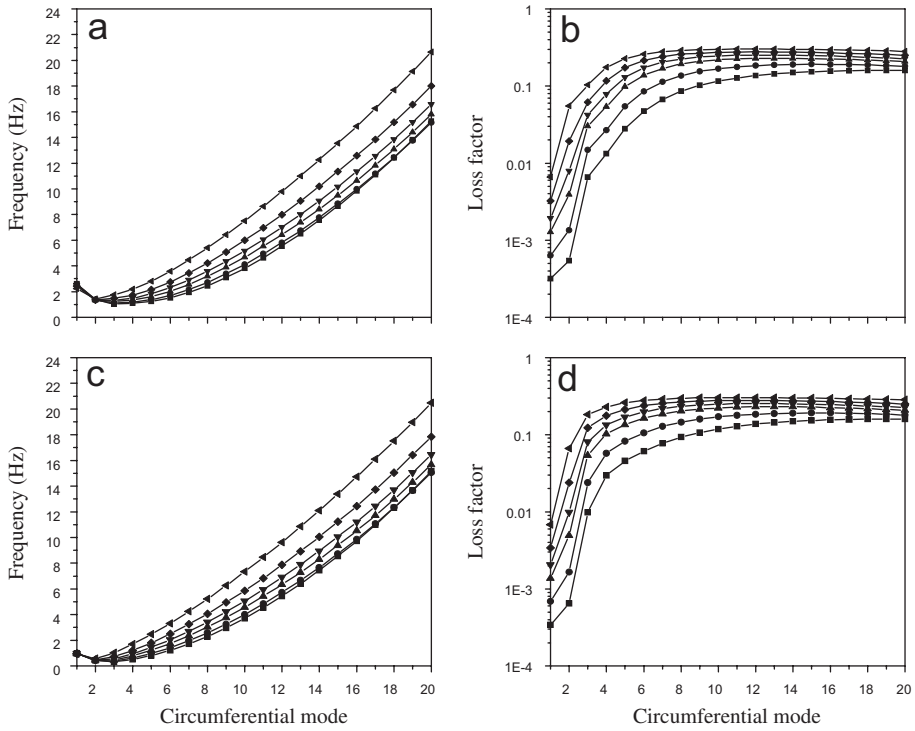


Fig. 6. Plot of frequency (Hz) and loss factor of a long Kevlar/Epoxy tank with fibre angle 90°: (a) frequencies of half-filled; (b) loss factors of half-filled; (c) frequencies of fully filled; (d) loss factors of fully filled: —■— $t_c/t_f = 0.5$; —●— $t_c/t_f = 1.0$; —▲— $t_c/t_f = 2.0$; —▼— $t_c/t_f = 3.0$; —♦— $t_c/t_f = 5.0$; —◀— $t_c/t_f = 10.0$.

Table 3
Comparison of frequencies (Hz) of different composite materials of a short fully-filled cylindrical shell with 0° fibre angle

| $m$ | Boron/Epoxy | | Glass/Epoxy | | Graphite/Epoxy | | Kevlar/Epoxy | |
|---|---|---|---|---|---|---|---|---|
| | $t_c/t_f = 1$ | $t_c/t_f = 5$ | $t_c/t_f = 1$ | $t_c/t_f = 5$ | $t_c/t_f = 1$ | $t_c/t_f = 5$ | $t_c/t_f = 1$ | $t_c/t_f = 5$ |
| 1 | 1.881 | 1.892 | 1.337 | 1.359 | 1.588 | 1.610 | 1.086 | 1.112 |
| 2 | 1.549 | 1.555 | 1.196 | 1.207 | 1.490 | 1.503 | 0.944 | 0.962 |
| 3 | 1.269 | 1.276 | 1.016 | 1.024 | 1.319 | 1.329 | 0.797 | 0.814 |
| 4 | 1.074 | 1.089 | 0.865 | 0.875 | 1.158 | 1.170 | 0.683 | 0.704 |
| 5 | 0.937 | 0.966 | 0.746 | 0.764 | 1.025 | 1.047 | 0.600 | 0.629 |
| 6 | 0.838 | 0.896 | 0.653 | 0.691 | 0.921 | 0.960 | 0.538 | 0.584 |
| 7 | 0.766 | 0.872 | 0.581 | 0.655 | 0.838 | 0.910 | 0.491 | 0.565 |
| 8 | 0.717 | 0.896 | 0.528 | 0.659 | 0.775 | 0.898 | 0.458 | 0.576 |
| 9 | 0.690 | 0.965 | 0.493 | 0.704 | 0.729 | 0.926 | 0.437 | 0.615 |
| 10 | 0.683 | 1.076 | 0.477 | 0.787 | 0.701 | 0.994 | 0.428 | 0.684 |

of a tall shell, the loss factors obtained for different boundary conditions are more or less same. In general, the simply supported shell seems to have higher damping compared to the CF shell and the CC shell.

### 4.2. Submerged viscoelastic cylindrical shell

#### 4.2.1. Validation

As explained in Section 3 the present methodology can be extended to submerged shells where subsequent change in spatial velocity potential is made by discarding the first kind of Bessel function $I_n$, as it must be

Table 4
Comparison of loss factors for different composite materials of a short fully filled cylindrical shell with 0° fibre angle

| $m$ | Boron/Epoxy | | Glass/Epoxy | | Graphite/Epoxy | | Kevlar/Epoxy | |
|---|---|---|---|---|---|---|---|---|
| | $t_c/t_f = 1$ | $t_c/t_f = 5$ | $t_c/t_f = 1$ | $t_c/t_f = 5$ | $t_c/t_f = 1$ | $t_c/t_f = 5$ | $t_c/t_f = 1$ | $t_c/t_f = 5$ |
| 1 | 0.0039 | 0.0106 | 0.0034 | 0.0122 | 0.0058 | 0.0158 | 0.0054 | 0.0187 |
| 2 | 0.0027 | 0.0092 | 0.0021 | 0.0087 | 0.0038 | 0.0124 | 0.0036 | 0.0151 |
| 3 | 0.0026 | 0.0107 | 0.0016 | 0.0077 | 0.0029 | 0.0115 | 0.0031 | 0.0151 |
| 4 | 0.0030 | 0.0137 | 0.0015 | 0.0081 | 0.0028 | 0.0127 | 0.0032 | 0.0172 |
| 5 | 0.0037 | 0.0179 | 0.0016 | 0.0094 | 0.0031 | 0.0151 | 0.0035 | 0.0200 |
| 6 | 0.0046 | 0.0237 | 0.0017 | 0.0116 | 0.0036 | 0.0187 | 0.0040 | 0.0230 |
| 7 | 0.0056 | 0.0319 | 0.0019 | 0.0156 | 0.0042 | 0.0238 | 0.0045 | 0.0262 |
| 8 | 0.0069 | 0.0430 | 0.0024 | 0.0220 | 0.0050 | 0.0307 | 0.0051 | 0.0295 |
| 9 | 0.0087 | 0.0566 | 0.0031 | 0.0304 | 0.0060 | 0.0395 | 0.0057 | 0.0332 |
| 10 | 0.0113 | 0.0713 | 0.0045 | 0.0397 | 0.0074 | 0.0498 | 0.0064 | 0.0375 |

Table 5
Comparison of frequencies (Hz) for different composite materials of a long fully filled cylindrical shell with $0^0$ fibre angle

| $m$ | Boron/Epoxy | | Glass/Epoxy | | Graphite/Epoxy | | Kevlar/Epoxy | |
|---|---|---|---|---|---|---|---|---|
| | $t_c/t_f = 1$ | $t_c/t_f = 5$ | $t_c/t_f = 1$ | $t_c/t_f = 5$ | $t_c/t_f = 1$ | $t_c/t_f = 5$ | $t_c/t_f = 1$ | $t_c/t_f = 5$ |
| 1 | 1.764 | 1.745 | 1.424 | 1.408 | 1.924 | 1.907 | 1.125 | 1.112 |
| 2 | 1.124 | 1.123 | 0.845 | 0.815 | 1.245 | 1.236 | 0.725 | 0.723 |
| 3 | 0.836 | 0.906 | 0.536 | 0.594 | 0.897 | 0.936 | 0.536 | 0.570 |
| 4 | 0.705 | 1.012 | 0.425 | 0.684 | 0.711 | 0.928 | 0.435 | 0.623 |
| 5 | 0.735 | 1.398 | 0.464 | 1.018 | 0.674 | 1.209 | 0.442 | 0.876 |
| 6 | 0.927 | 1.962 | 0.622 | 1.486 | 0.784 | 1.687 | 0.562 | 1.236 |
| 7 | 1.254 | 2.652 | 0.863 | 2.051 | 1.021 | 2.288 | 0.725 | 1.772 |
| 8 | 1.648 | 3.245 | 1.142 | 2.703 | 1.347 | 2.978 | 0.965 | 2.356 |
| 9 | 2.125 | 4.175 | 1.522 | 3.431 | 1.744 | 3.741 | 1.277 | 3.026 |
| 10 | 2.669 | 5.036 | 1.933 | 4.228 | 2.203 | 4.564 | 1.625 | 3.768 |

Table 6
Comparison of loss factors for different materials of a long fully filled cylindrical shell with 0° fibre angle

| $m$ | Boron/Epoxy | | Glass/Epoxy | | Graphite/Epoxy | | Kevlar/Epoxy | |
|---|---|---|---|---|---|---|---|---|
| | $t_c/t_f = 1$ | $t_c/t_f = 5$ | $t_c/t_f = 1$ | $t_c/t_f = 5$ | $t_c/t_f = 1$ | $t_c/t_f = 5$ | $t_c/t_f = 1$ | $t_c/t_f = 5$ |
| 1 | 0.00033 | 0.00170 | 0.00036 | 0.00191 | 0.00031 | 0.00154 | 0.00071 | 0.00368 |
| 2 | 0.00045 | 0.00266 | 0.00032 | 0.00186 | 0.00033 | 0.00195 | 0.00072 | 0.00408 |
| 3 | 0.00081 | 0.01160 | 0.00042 | 0.00710 | 0.00048 | 0.00593 | 0.00079 | 0.00662 |
| 4 | 0.00374 | 0.04696 | 0.00234 | 0.02956 | 0.00168 | 0.02653 | 0.00148 | 0.01861 |
| 5 | 0.01373 | 0.08884 | 0.00825 | 0.05246 | 0.00682 | 0.05848 | 0.00439 | 0.03607 |
| 6 | 0.02807 | 0.12144 | 0.01564 | 0.07269 | 0.01618 | 0.08586 | 0.00923 | 0.05246 |
| 7 | 0.04155 | 0.14766 | 0.02165 | 0.09235 | 0.02588 | 0.10896 | 0.01453 | 0.06831 |
| 8 | 0.05364 | 0.16970 | 0.02789 | 0.11169 | 0.03476 | 0.12983 | 0.01901 | 0.08423 |
| 9 | 0.06522 | 0.18881 | 0.03472 | 0.12997 | 0.04329 | 0.14903 | 0.02392 | 0.10003 |
| 10 | 0.07678 | 0.20495 | 0.04196 | 0.14682 | 0.05190 | 0.16639 | 0.02910 | 0.11533 |

regular at extreme radius. Table 11 lists the natural frequencies—of a submerged shell whose dimensions are $R = 0.175$, $L = 0.664$ and $t = 0.001$ m which is simply supported at both ends—obtained by the present approach and from the work of Amabili [7]. The correlation observed is good.

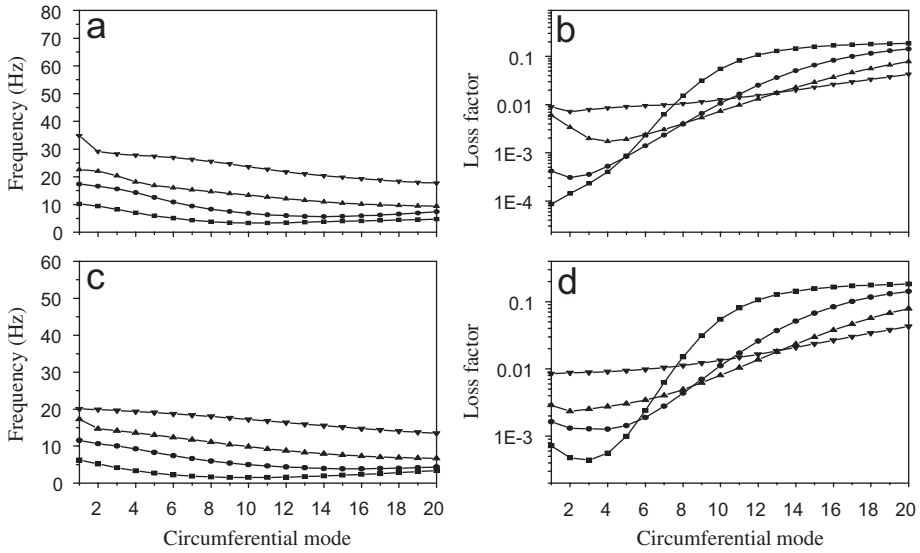


Fig. 7. Frequencies (Hz) and loss factors of a short mild steel cylindrical shell for higher axial modes for $t_c/t_f = 1$: (a) frequencies of half-filled; (b) loss factors of half-filled; (c) frequencies of fully filled; (d) loss factors of fully filled: —■— $n = 1$; —●— $n = 2$; —▲— $n = 3$; —▼— $n = 5$.

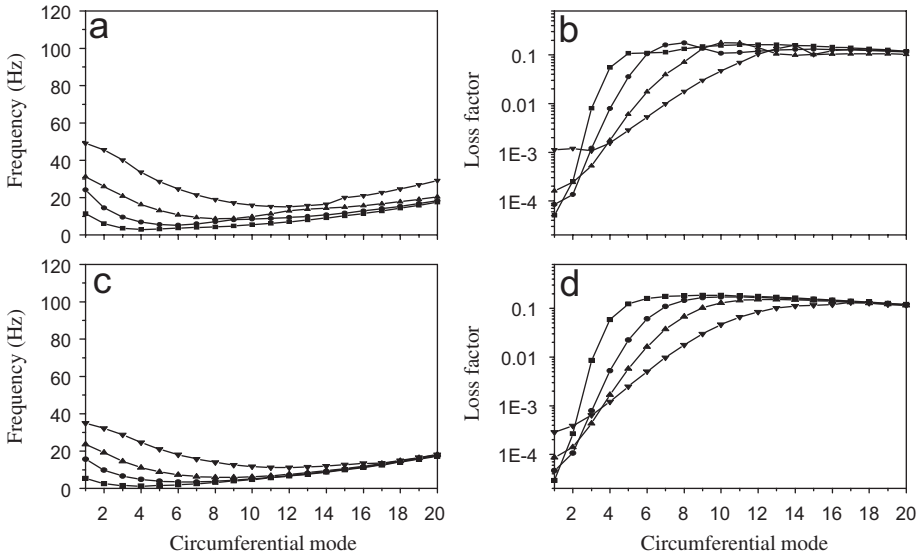


Fig. 8. Frequencies (Hz) and loss factors of a long mild steel cylindrical shell for higher axial modes for $t_c/t_f = 1$: (a) frequencies of half-filled; (b) loss factors of half-filled; (c) frequencies of fully filled; (d) loss factors of fully filled: —■— $n = 1$; —●— $n = 2$; —▲— $n = 3$; —▼— $n = 5$.

The present methodology is also validated by selecting a circular cylindrical shell with different dimensions, which is clamped at one end while other end is free. The shell is made of stainless steel and has a radius of 0.07654 m, length of 1.35 m, and wall thickness of 0.002286 m. The material properties of the shell are as follows. Young's modulus is $200 \times 10^9\,\mathrm{N\,m^{-2}}$, Poisson's ratio is 0.3, and mass density is $7850\,\mathrm{kg\,m^{-3}}$. The density of liquid in the shell is $1000\,\mathrm{kg\,m^{-3}}$. The natural frequencies of the shell are calculated by the present method and are compared with those reported by Maguire [8],

Table 7
Comparison of frequencies (Hz) of a fluid-filled short mild shell for different boundary conditions

| $m$ | First axial mode ($n = 1$) | | |
|---|---|---|---|
| | CC | SS | CF |
| 1 | 7.0392 | 6.6014 | 6.2453 |
| 2 | 7.0250 | 6.7990 | 5.2110 |
| 3 | 6.6525 | 6.5143 | 4.1497 |
| 4 | 6.1376 | 5.9005 | 3.3181 |
| 5 | 5.6204 | 5.1874 | 2.6931 |
| 6 | 5.1500 | 4.5111 | 2.2286 |
| 7 | 4.7366 | 3.9239 | 1.8925 |
| 8 | 4.3784 | 3.4370 | 1.6650 |
| 9 | 4.0711 | 3.0467 | 1.5344 |
| 10 | 3.8116 | 2.7459 | 1.4908 |

Table 8
Comparison of loss factors of a fluid-filled short mild shell for different boundary conditions

| $m$ | First axial mode ($n = 1$) | | |
|---|---|---|---|
| | CC | SS | CF |
| 1 | 0.00088 | 0.00100 | 0.00072 |
| 2 | 0.00073 | 0.00067 | 0.00047 |
| 3 | 0.00072 | 0.00039 | 0.00044 |
| 4 | 0.00087 | 0.00028 | 0.00056 |
| 5 | 0.00118 | 0.00040 | 0.00100 |
| 6 | 0.00174 | 0.00086 | 0.00241 |
| 7 | 0.00270 | 0.00197 | 0.00630 |
| 8 | 0.00433 | 0.00434 | 0.01517 |
| 9 | 0.00699 | 0.00893 | 0.03135 |
| 10 | 0.01119 | 0.01693 | 0.05462 |

Table 9
Comparison of frequencies (Hz) of a fluid-filled long mild shell for different boundary conditions

| $m$ | First axial mode ($n = 1$) | | |
|---|---|---|---|
| | CC | SS | CF |
| 1 | 10.6401 | 10.0784 | 12.2475 |
| 2 | 7.4579 | 5.5629 | 5.2494 |
| 3 | 5.4537 | 3.3783 | 2.9431 |
| 4 | 4.1760 | 2.3842 | 2.3791 |
| 5 | 3.4213 | 2.0581 | 2.7173 |
| 6 | 3.1114 | 2.1926 | 3.4005 |
| 7 | 3.1857 | 2.6175 | 4.1566 |
| 8 | 3.5561 | 3.2138 | 4.9449 |
| 9 | 4.1339 | 3.9240 | 5.7960 |
| 10 | 4.8581 | 4.7246 | 6.7254 |

Hoon and Lee [9]. The comparisons are listed in Table 12. The fluid surrounding the shell is bounded by a reservoir, which has an axially varying radius in the finite-element model of Maguire[1]. However, in the experimental work of Maguire[2] and also in the present approach, it is assumed that the shell is

Table 10
Comparison of loss factors of a fluid-filled long mild shell for different boundary conditions

| $m$ | First axial mode ($n = 1$) | | |
|---|---|---|---|
| | CC | SS | CF |
| 1 | 0.00004 | 0.00002 | 0.00002 |
| 2 | 0.00010 | 0.00009 | 0.00025 |
| 3 | 0.00076 | 0.00165 | 0.00838 |
| 4 | 0.00515 | 0.01493 | 0.05736 |
| 5 | 0.02207 | 0.05931 | 0.11850 |
| 6 | 0.05985 | 0.11850 | 0.14660 |
| 7 | 0.10810 | 0.15830 | 0.15651 |
| 8 | 0.14600 | 0.17731 | 0.16365 |
| 9 | 0.16709 | 0.18433 | 0.16870 |
| 10 | 0.17571 | 0.18494 | 0.17095 |

Table 11
Comparison of the natural frequencies (Hz) of a liquid surrounded shell

| $m$ | Amabili and Dalpiaz [7] | Present approach |
|---|---|---|
| | Frequency (Hz) | Frequency (Hz) |
| 1 | 94.80 | 109.13 |
| 2 | 135.99 | 137.07 |
| 3 | 236.00 | 228.27 |
| 4 | 528.36 | 493.35 |

Table 12
Comparison of natural frequencies of a shell surrounded with 90% of fluid

| $n$ | Partially liquid-surrounded shell (90% liquid level) | | | | |
|---|---|---|---|---|---|
| | Method | $m = 1$ | $m = 2$ | $m = 3$ | $m = 4$ |
| 1 | Maguire[1] | 42.2 | 137.7 | 389.9 | 824.2 |
| | Maguire[2] | — | 160.0 | 479.9 | — |
| | Hoon and Lee [9] | 56.6 | 168.7 | 479.7 | 987.3 |
| | Present study | 58.1 | 171.7 | 487.4 | 989.3 |
| 2 | Maguire[1] | 303.0 | 200.1 | 457.7 | 859.3 |
| | Maguire[2] | — | 205.5 | 531.9 | — |
| | Hoon and Lee [9] | 308.1 | 215.4 | 502.6 | 1012.8 |
| | Present study | 315.5 | 225.4 | 511.1 | 1012.3 |
| 3 | Maguire[1] | 892.0 | 404.7 | 576.2 | 942.5 |
| | Maguire[2] | — | 330.2 | 540.0 | — |
| | Hoon and Lee [9] | 756.8 | 345.6 | 557.6 | 1056.9 |
| | Present study | 773.3 | 360.8 | 571.1 | 1048.2 |
| 4 | Maguire[1] | 1354.0 | 618.3 | 736.8 | 1081.0 |
| | Maguire[2] | — | 545.9 | 618.7 | — |
| | Hoon and Lee [9] | 1295.3 | 569.6 | 643.3 | 1124.0 |
| | Present study | 1323.2 | 593.5 | 671.7 | 1098.2 |
| 5 | Maguire[1] | 1962.0 | 959.8 | 804.8 | 1262.0 |
| | Maguire[2] | — | — | 719.5 | — |
| | Hoon and Lee [9] | 1876.6 | 856.9 | 739.5 | 1214.9 |
| | Present study | 1921.4 | 899.2 | 780.4 | 1195.5 |

surrounded with a radially infinite exterior liquid. This difference might result in small discrepancy between the natural frequencies obtained by the present method and the finite-element results of Maguire[1]. It is found that the natural frequencies of the liquid-surrounded shell with the assumption of infinite fluid domain (by Hoon and Lee) and from the present method agree well with the experimental results of Maguire[2].

*4.2.2. Studies on submerged isotropic short and long shells*

Studies are carried out to analyse submerged isotropic shells for free vibration and damping characteristics. The dimensions of a short cylindrical shell are $R = 18.29$, $L = 12.2$, $t = 0.0254$ and long shell dimensions are $R = 7.34$, $L = 21.96$, $t = 0.0254$ m. Fig. 9 illustrates the natural frequencies and loss factors of a short mild steel tank when surrounded by water. The frequency behaviour and loss factor is observed to be similar to fluid-filled viscoelastic shell (see Section 4.1.2). In case of half-surrounded shells, for the first few circumferential modes frequencies decrease with the increase in the $t_c/t_f$ ratio. This is mainly because the mass effects dominate in the case of shell vibration. Lowest frequency occurs when mass effects and bending effects are equal. Once the lowest frequency is crossed, then the frequency increases with increase in $t_c/t_f$ ratio, as bending effects are predominant at higher circumferential modes. However, when compared to fluid-filled shell, submerged shell's bending mode frequency is higher. This is due the effect of hoop stress, which would make the shell stiffer in bending modes. There was no significant difference in the case of loss factor of half-surrounded shell and half-filled shell; however, loss factor of fully surrounded shell is slightly higher than that of fully filled shell.

Fig. 10 shows the natural frequencies and loss factor of a typical long shell when it is surrounded with water. The frequency behaviour observed is similar to long shells (refer Section 4.1.2.). However, the loss factors of

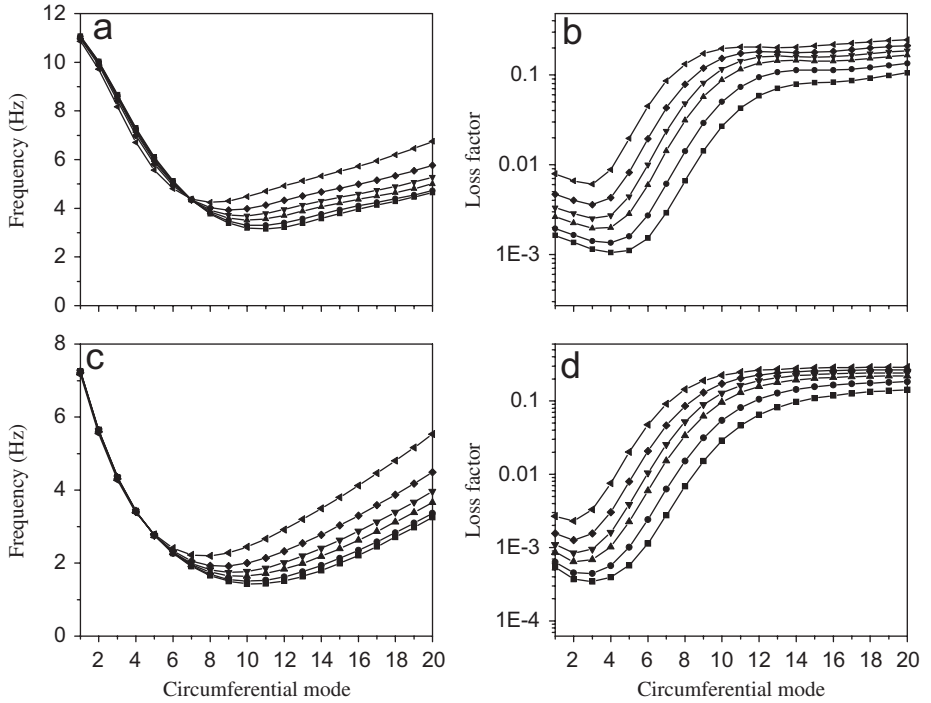


Fig. 9. Plot of frequency (Hz) and loss factor of a short mild steel fluid surrounded shell: (a) frequencies of half-filled; (b) loss factors of half-filled; (c) frequencies of fully filled; (d) loss factors of fully filled: —■— $t_c/t_f = 0.5$; —●— $t_c/t_f = 1.0$; —▲— $t_c/t_f = 2.0$; —▼— $t_c/t_f = 3.0$; —◆— $t_c/t_f = 5.0$; —◀— $t_c/t_f = 10.0$.

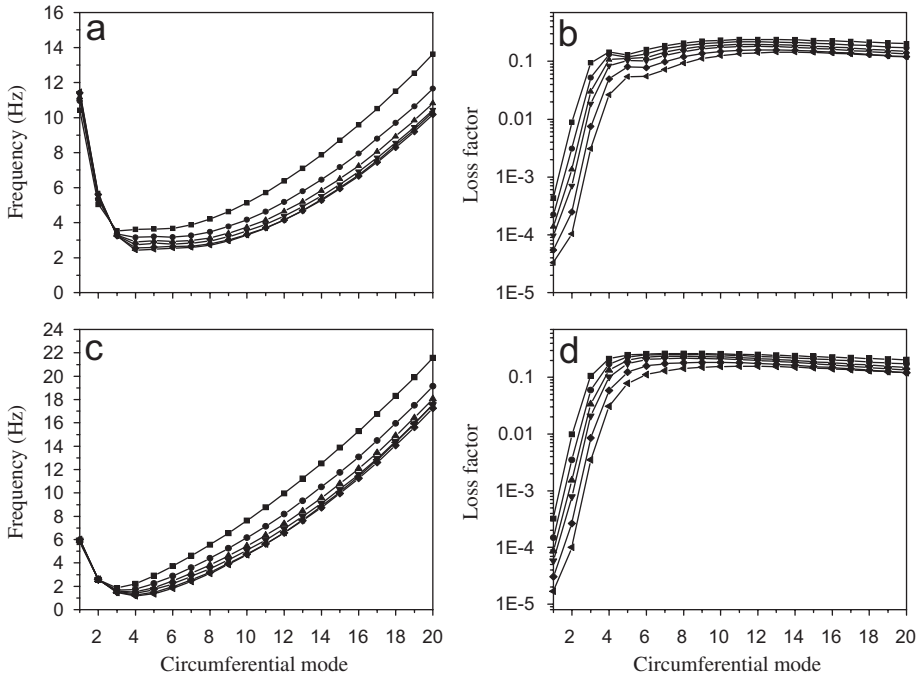


Fig. 10. Plot of frequency (Hz) and loss factor of a long mild steel fluid surrounded shell: (a) frequencies of half-filled; (b) loss factors of half-filled; (c) frequencies of fully filled; (d) loss factors of fully filled: —■— $t_c/t_f = 0.5$; —●— $t_c/t_f = 1.0$; —▲— $t_c/t_f = 2.0$; —▼— $t_c/t_f = 3.0$; —◆— $t_c/t_f = 5.0$; —◀— $t_c/t_f = 10.0$.

both half-surrounded and fully surrounded are slightly higher than the half-filled and fully filled cylindrical shells respectively.

*4.2.3. Orthotropic submerged shells*

Fig. 11 shows the natural frequencies and loss factor of a short Kevlar/Epoxy shell with axial fibre orientation and surrounded with fluid. It is seen that the fall in frequency due to the external fluid effect in composite shells are much higher compared to composite fluid-filled cylindrical shells. In most of the cases damping in fluid surrounded shells are marginally higher than that of fluid-filled shells for higher circumferential modes. Damping of fluid-filled shells is higher for axisymmetric mode and first bending mode especially when compared to fluid surrounded shell.

Fig. 12 shows the natural frequencies and loss factor of a long Kevlar/Epoxy shell with axial fibre orientation and surrounded with fluid. The trend observed is similar to that of Fig. 11. It is also observed that frequencies of short Glass/Epoxy shell with fluid surrounded and fluid-filled shell are in the same range except for the higher circumferential modes where fluid surrounded shell has higher natural frequency. In the case of loss factors, the fluid surrounded shell seems to have higher amount of damping throughout the range. The above results and comments hold good also for composite shell with circumferential fibre orientation.

## 5. Partially liquid-filled and partially submerged shells

Studies are extended to both partially liquid-filled and partially submerged shells by algebraically adding the added-masses of submerged and fluid-filled cases, and results are compared with the only work found in this area by Chiba [4] in Table 13. The shell is clamped at one end and other end is free. Shell is made up of polyster film with the geometrical parameter $z = L^2\sqrt{1-\nu^2}/Rt = 502$. The liquid is water. The radius of shell is $R = 0.1$ m, the thickness is $t = 0.244$ mm, the length is $L = 0.1131$ m, and the radius of the outer

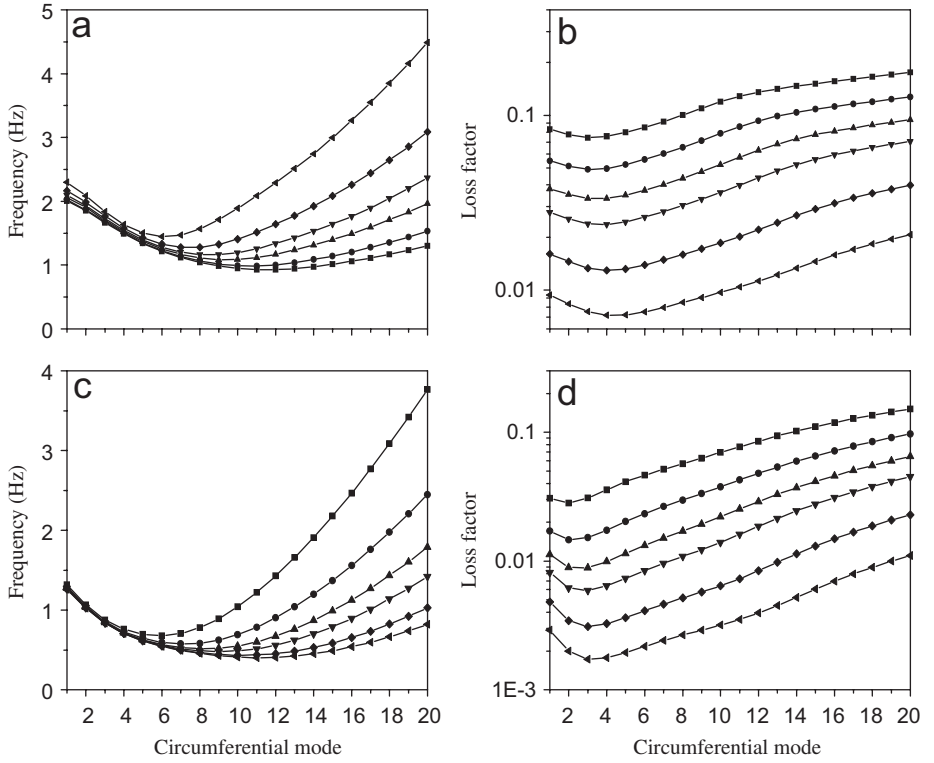


Fig. 11. Plot of frequency (Hz) and loss factor of a short Kevlar/Epoxy fluid surrounded shell with 0° fibre orientation: (a) frequencies of half-filled; (b) loss factors of half-filled; (c) frequencies of fully filled; (d) loss factors of fully filled: —■— $t_c/t_f = 0.5$; —●— $t_c/t_f = 1.0$; —▲— $t_c/t_f = 2.0$; —▼— $t_c/t_f = 3.0$; —◆— $t_c/t_f = 5.0$; —◀— $t_c/t_f = 10.0$.

cylinder is $R_0 = 0.195$ m. A good correlation in the trend for the variation of frequency is observed. However, the discrepancy at higher modes may be due to the fact that the results from the present study are obtained for infinite liquid domain where as the results reported by Chiba [4] are for finite liquid domain. Studies can be extended to fluid-filled as well as fluid surrounded viscoelastic shells for different boundary conditions.

## 6. Conclusions

A generalised method is proposed in this paper for the frequency analysis of conventional viscoelastic fluid-filled or fluid surrounded shells. The method consists of treating fluid domain with Bessel function approach and shell domain using finite-element discretisation. The present approach obviates the discretisation of liquid domain thus reducing the computation time. The proposed method overcomes most of the limitations suffered by adopting approaches suggested in the literature. Results of frequency analysis obtained using this method correlate very well with those obtained using other approaches found in the literature for solving diverse fluid–shell problems. Hence, it is claimed that the present approach is numerically robust and can be easily used for different configurations—fluid-filled or submerged, any amount of fluid filling, boundary condition—of fluid–shell interaction problems.

In the present paper, numerical results are presented for isotropic as well as orthotropic viscoelastic shell structures. The response of the viscoelastic fluid-filled or fluid-surrounded shells at resonance will be lower compared to conventional mild steel systems as damping present in the system is higher. Observing that the loss factors—a metric that is proportional to the amount of damping present in the fluid–shell system—for these shell structures are substantially high, one could confidently draw the above conclusion. In case of

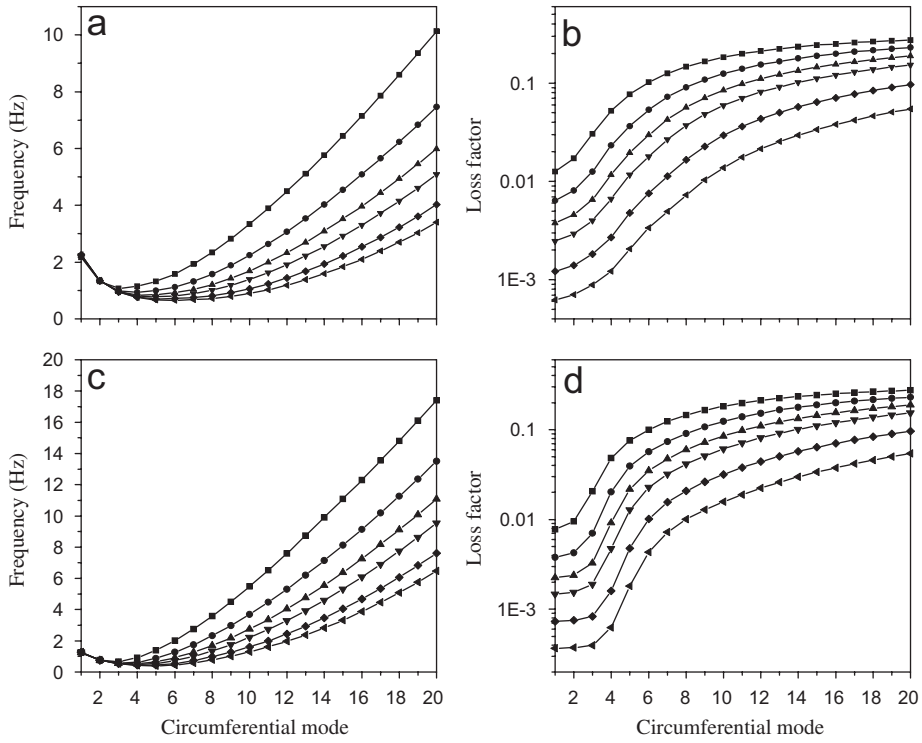


Fig. 12. Plot of frequency (Hz) and loss factor of a long Kevlar/Epoxy fluid surrounded shell with 0° fibre orientation: (a) frequencies of half-filled; (b) loss factors of half-filled; (c) frequencies of fully filled; (d) loss factors of fully filled: —■— $t_c/t_f = 0.5$; —●— $t_c/t_f = 1.0$; —▲— $t_c/t_f = 2.0$; —▼— $t_c/t_f = 3.0$; —◆— $t_c/t_f = 5.0$; —◀— $t_c/t_f = 10.0$.

Table 13
Natural frequencies (Hz) of completely filled and completely submerged shell polyster film with the geometrical parameter $z = 502$

| Circumferential mode | Present approach | Chiba [4] |
|---|---|---|
| 1 | 140.96 | 140 |
| 2 | 80.55 | 82 |
| 3 | 50.89 | 58 |
| 4 | 34.79 | 40 |
| 5 | 25.46 | 31 |

The inner and outer radii of shell are $R = 0.1$ m, $R_0 = 0.195$ m, the thickness is $t = 0.244$ mm, the length is $L = 0.1131$ m.

orthotropic shells, the effect of fibre orientation is examined. It is found that for shells with axial fibre orientation the added mass effect of fluid is less for lower circumferential modes and increases for higher circumferential modes. In case of shells with circumferential fibre orientation the added mass effect of fluid is more predominant than shells with axial fibre orientation; this observation holds good for both fluid-surrounded and fluid-filled shells. In general, fluid-filled shells have slightly higher natural frequency when compared to fluid-surrounded shells.

## Appendix A

Material properties used in the present study (see Table A1).

Table A1
Material properties used in the present study

| | |
|---|---|
| i. | PVC<br>E1 = E2 = E3 = (2.3E7, i.0.782E7) N/m$^2$, $\nu_{12} = \nu_{13} = \nu_{23} = 0.34$, $\rho = 1340\,kg/m^3$ |
| ii. | Mild steel<br>E1 = E2 = E3 = 2.04E11 N/m$^2$, $\nu_{12} = \nu_{13} = \nu_{23} = 0.3$ and $\rho = 7800\,kg/m^3$ |
| iii. | Glass/Epoxy<br>E1 = 38.60E9, E2 = 8.27E9, G12 = 4.14E9 N/m$^2$, $\nu_{12} = 0.26$, $\rho = 1810\,kg/m^3$, E3 = E2, G13 = G12, G23 = G12, $\nu_{13} = \nu_{12}$,$\nu_{23} = \nu_{12}$ |
| iv. | Boron/Epoxy<br>E1 = 204E9, E2 = 18.3E9, G12 = 5.5E9 N/m$^2$, $\nu_{12} = 0.23$, $\rho = 2000\,kg/m^3$, E3 = E2, G13 = G12, G23 = G12, $\nu_{13} = \nu_{12}$, $\nu_{23} = \nu_{12}$ |
| v. | Kevlar/Epoxy<br>E1 = 76E9, E2 = 5.5E9, G12 = 2.3E9 N/m$^2$, $\nu_{12} = 0.34$, $\rho = 1460\,kg/m^3$, E3 = E2, G13 = G12, G23 = G12, $\nu_{13} = \nu_{12}$, $\nu_{23} = \nu_{12}$ |
| vi. | Graphite/Epoxy<br>E1 = 184.5E9, E2 = 10.91E9, G12 = 7.31E9 N/m$^2$, $\nu_{12} = 0.28$, $\rho = 1600\,kg/m^3$, E3 = E2, G13 = G12, G23 = G12, $\nu_{13} = \nu_{12}$, $\nu_{23} = \nu_{12}$ |

## References


[1] M.A. Haroun, Vibration studies and tests of liquid storage tanks, *Earthquake Engineering and Structural Dynamics* 11 (1) (1983) 179–206.

[2] R.K. Gupta, G.L. Hutchinson, Free vibration analysis of liquid storage tanks, *Journal of Sound and Vibration* 123 (1988) 491–506.

[3] R. Ramasamy, N. Ganesan, Finite element analysis of fluid filled isotropic cylindrical shells with constrained viscoelastic damping, *Computers & Structures* 70 (1998) 363–376.

[4] M. Chiba, Free vibration of a partially liquid-filled and partially submerged, clamped–free circular cylinder shell, *Journal of Acoustical Society of America* 100 (4) (1996) 2170–2180.

[5] D.J. Wilkins Jr., C.W. Bert, D.M. Egle, Vibrations of orthotropic sandwich conical shells with various boundary conditions, *Journal of Sound and Vibration* 13 (1970) 211–228.

[6] J.C. Luke, A variational principle for a liquid with free surface, *Journal of Fluid Mechanics* 27 (1967) 395–397.

[7] M. Amabili, G. Dalpiaz, Breathing vibrations of a horizontal circular cylindrical tank shell, partially filled with liquid, *Journal of Sound and Vibration* 117 (1995) 187–191.

[8] J.R. Maguire, A study of cylindrical shell vibrations in fluid, *Proceedings of the Institution of Mechanical Engineers, Flow Induced Vibrations, International Conference, IMechE*, 1991, pp. 321–331.

[9] K.-J. Hoon, S.-C. Lee, Fourier series expansion method for free vibration analysis of either a partially liquid-filled or a partially liquid-surrounded circular cylindrical shell, *Computer & Structures* 58 (5) (1995) 937–946.